Materials Science and Engineering C 59 (2016) 438–444

Contents lists available at ScienceDirect

Materials Science and Engineering C

journal homepage: www.elsevier.com/locate/msec

Development of ammonia sensors by using conductive polymer/hydroxyapatite composite materials

Li Huixia, Liu Yong *, Luo Lanlan, Tan Yanni *, Zhang Qing, Li Kun

State Key Laboratory of Powder Metallurgy, Central South University, 932 Lushan South Road, Changsha 410083, PR China

ARTICLE INFO

Article history:
Received 4 August 2015
Received in revised form 14 September 2015
Accepted 14 October 2015
Available online 23 October 2015

Keywords:
Ammonia
Hydroxyapatite
Polypyrrole
Polyaniline
Gas sensing property

ABSTRACT

In order to improve the gas sensing properties, hydroxyapatite (HAp)-based composites were prepared by mixing with different contents of conductive polymers: polypyrrole (PPy) and polyaniline (PAni). The compositions, microstructures and phase constitutions of polymer/HAp composites were characterized, and the sensing properties were studied using a chemical gas sensing (CGS-8) system. The results showed that, compared to pure HAp, the sensitivities of the composites to ammonia were improved significantly. 5%PPy/HAp and 20%PAni/HAp composites exhibited the best sensitivities to ammonia, and the sensitivities at 500 ppm were 86.72% and 86.18%, respectively. Besides, the sensitivity of 5%PPy/HAp at 1000 ppm was up to 90.7%. Compared to pure PPy and PAni, the response and the recovery time of 5%PPy/HAp and 20%PAni/HAp at 200 ppm were shortened several times, and they were 24 s/245 s and 15 s/54 s, respectively. In addition, the composites showed a very high selectivity to ammonia. The mechanism for the enhancement of the sensitivity to ammonia was also discussed. The polymer/HAp composites are very promising in applications of ammonia sensors.

1. Introduction

Ammonia, a poisonous gas with a pungent stench, can endanger the health and safety of human body after an excessive inhalation. The smell detection limit of human body to ammonia is about 50 ppm, and it may take about 24 h before the unpleasant symptoms develop. Therefore, the detection of ammonia in a trace level is important since the leakage of ammonia in chemical industry, vehicle and combustion systems has become an un-negligible problem. The Occupational Safety and Health Administration (OSHA) has set an acceptable limit of 25 ppm of ammonia at an exposure of 8 h and a short-term (15 min) exposure level of 35 ppm for human beings at the workplace [1,2]. Inorganic metal oxide semiconductors, like ZnO [3], TiO_2 [4], WO_3, Cr_2O_3 and In_2O_3 [5], have been applied as sensor materials for ammonia, but their operation temperatures are often above 300 °C. Even though some composite films are developed to measure ammonia at room temperature, the sensitivity is relatively low and the lack of selectivity is still a difficult problem to handle [6].

Since iodine-doped polyacetylene with high conductivity was found by Shirakawa in 1977, conductive polymers including polyaniline (PAni), polypyrrole (PPy) and polythiophene (PT) et al. have been extensively explored recent years due to their excellent chemical and physical properties originating from their unique π-conjugated system. They are easy to be synthesized and processed, and have high electrical conductivity and long term environmental stability, which make them useful in electronic, optoelectronic and electromechanical filed. One of the most popular applications is sensors. For example, conductive polymers have been used to fabricate composites biosensors with CNTs [7,8] and Fe_3O_4 [9,10] for the detection of H_2O_2 [11] and glucose [12], which exhibit high sensitivity and low detection limit. PPy [13] and PAni [14] are the most frequently used and studied polymers for sensing ammonia, the sensing properties can be measured at room temperature. However, the sensitivity and the selectivity of PPy and PAni to ammonia prepared by chemical oxidative polymerization are lower than those prepared by the electrochemical deposition, and the response time and the recovery time are very long. Besides, the irreversibility and the insolubility are serious problems remained to be solved [15,16]. To combine the properties of pure organic and inorganic materials for gas sensor applications, composite materials such as PPy/WO_3 [17], PPy/SnO_2 [18,19], PPy/ZnO [20], PPy/Fe_2O_3 [21], PPy/MoO_3 [22], PPy/NiO [23] PAni/SnO_2 [24,25] and PAni/TiO_2 [26–31] have been developed to improve the gas sensing properties to H_2S, NH_3 and NO_2. Although the sensitivity, reversibility and response/recovery time for ammonia are improved compared to pure PPy and PAni, the recovery time of the composites is still as long as hundreds of seconds. Besides, the sensitivities of the sensing materials can barely reach 90% and there is still about 10% of shift of the initial value after several cycles of measurement.

In our previous work, the tubular hydroxyapatite (HAp) prepared by an electrochemical deposition method assisted with a cation exchange membrane showed excellent sensing properties to ammonia, and the sensing mechanisms to ammonia were proposed [32]. In this paper,

* Corresponding authors.
E-mail addresses: huixialee1990@163.com (L. Huixia), yonliu@csu.edu.cn (L. Yong), luolanlan1991@163.com (L. Lanlan), tanyanni@csu.edu.cn (T. Yanni), zhts0211@hotmail.com (Z. Qing), kunlee@csu.edu.cn (L. Kun).

http://dx.doi.org/10.1016/j.msec.2015.10.036
0928-4931/

PPy and PAni were used to be mixed with tubular HAp to further enhance the sensing properties to ammonia. The sensitivity, response/recovery time, selectivity of pure PPy, PAni, HAp, PPy/HAp composites and PAni/HAp composites to ammonia were studied. Besides, the sensing mechanisms of the polymer/HAp composites to ammonia were discussed.

2. Materials and methods

The Nafion N-117 cation-exchange membrane, $Ca(NO_3)_2 \cdot 4H_2O$ and $NH_4H_2PO_4$ were purchased from Alfa Aesar. All other chemicals (such as $NH_3 \cdot H_2O$, $NH_4S_2O_4$, HCl and N,N'-dimethyl formamide (DMF)) were of analytical reagent grade, and used as received unless otherwise noted. Pyrrole (Py) and aniline (Ani) were distilled under reduced pressure, put in a desiccator and stored in the refrigerator (0–4 °C). Deionized water (DI water) was produced by ULUP-1–20 T.

PPy and PAni were prepared by a chemical oxidative polymerization method at room temperature. The volume ratios of pyrrole and aniline monomers to the oxidant of $NH_4S_2O_4$ were 1:1, respectively. 1 mol/L HCl was used to add H^+ to PPy and PAni. The tubular HAp was fabricated using an electrochemical deposition method assisted with a cation exchange membrane, followed by stewing at 50 °C for 7 days [32–34]. The microstructures and compositions of the samples were characterized by Scanning electron microscopy (SEM), transmission electron microscopy (TEM), X-ray diffraction (XRD) and Fourier transform infrared spectroscopy (FT-IR) analyses, respectively.

Organic–inorganic composite materials of PPy/HAp and PAni/HAp were prepared by mechanically mixing. PPy, PAni and HAp were dispersed in N,N'-dimethyl formamide (DMF), respectively, and the HAp suspension was added into the PPy and PAni suspensions dropwise, then the mixed suspension was stirred continuously for 24 h at room temperature. According to the different mass content of polymer, the obtained composites were described as 2.5%PPy/HAp, 5%PPy/HAp, 10%PPy/HAp, 1%PAni/HAp, 5%PAni/HAp, 10%PAni/HAp, 20%PAni/HAp, 30%PAni/HAp and 50%PAni/HAp, respectively.

Gas sensing properties were measured by a CGS-8 (Chemical gas sensor-8) intelligent gas sensing analysis system (Beijing Elite Tech Co., Ltd., China). In the gas-sensing tests, ammonia was selected as the major target gas at room temperature. PPy, PAni, HAp, PPy/HAp and PAni/HAp composites were coated on a ceramic tube with 4 Au electrodes. A Ni–Cr alloy wire was used as a heating filament across the tube. All the gas sensing properties were measured in a 1 dm^3 glass bottle. Firstly, the bottle was vacuumed, and injected with a certain amount of ammonia. After the ammonia diffused absolutely in the bottle, the air was allowed to enter and mix homogeneously. Secondly, the gas sensor was put into the bottle immediately, and the electric resistance of the sensor changed rapidly. When the resistance reached a stable level, the sensor was taken out, and the resistance came back to the initial value. The sensitivity was defined as $S = (Ra–Rg)/Ra * 100\%$, where Ra and Rg were the resistances of the sensor in ambient air and target gas, respectively. The response time and the recovery time of the sensor were the time required for a change in the resistance of the sensor to reach 90% of the equilibrium value after injecting and removing the target gases, respectively. The resistance of the sensor was measured according to the schematic diagram, as shown in Fig. 1. The working temperature of the sensor could be controlled by adjusting the heating current across the resistor inside the ceramic tube. Since the sensing properties of the sensors in the experiments were measured at room temperature, the current value was zero. Reference resistors which could automatically select were put in series with the sensor to form a complete measuring circuit. According to the working voltage and the resistance of the reference resistors, we knew the current of the measuring circuit. Then the resistance of the sensor could be calculated.

3. Results and discussions

Fig. 2 shows the XRD patterns of PPy, PAni, HAp, 10%PPy/HAp, 50%PAni/HAp composite. Pure PPy has a broad, amorphous diffraction peak centered at about $2\theta = 26°$. PAni exhibits a certain degree of crystallinity, and shows similar strong peaks at $2\theta = 20.44°$ and 25.1°, corresponding to (100) and (110) planes, respectively. For HAp, all the diffraction peaks can be indexed as a pure hexagonal phase with a space group of P63/m, in consistence with the standard patterns of HAp (PDF 09-0432). The sharp peak at $2\theta = 25.9°$ indicates a good crystallization and growth preference on the (002) crystal plane. In addition, the HAp has a crystallinity of 86.87% according to the calculation. However, the peaks of PPy and PAni cannot be seen obviously in the XRD patterns of the composites. It may be because the diffraction peaks of PPy and PAni are weak and covered by the background of the HAp peaks.

Fig. 3 shows the SEM images of HAp (a), PPy (b), PAni (c), PPy/HAp composite (g), PAni/HAp composite (j) and TEM images of HAp (d), PPy (e), PAni (f), PPy/HAp composite (h), PAni/HAp composite (i). HAp shows a tubular structure with a diameter of 2.5–5 μm, and a length of 5–20 μm (Fig. 3(a)). In the TEM image, it can be seen that the tubular HAp consists of nanorods (Fig. 3(d)). HAp nanorods aggregate in a certain orientation to form clusters and then form tubular HAp after a process of self-assembly with the assist of cation-exchange membrane. PPy exhibits a uniform spherical morphology (Fig. 3(b)). The diameter

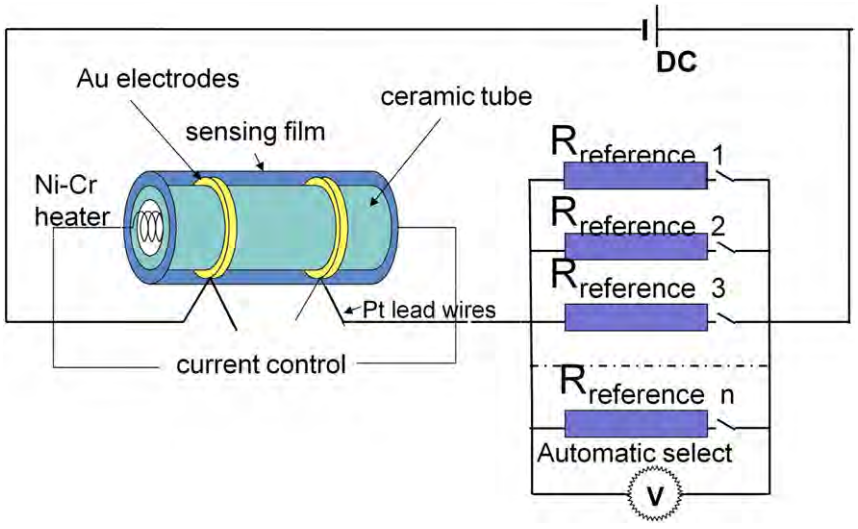

Fig. 1. Schematic diagram of the resistance measurement of sensors.

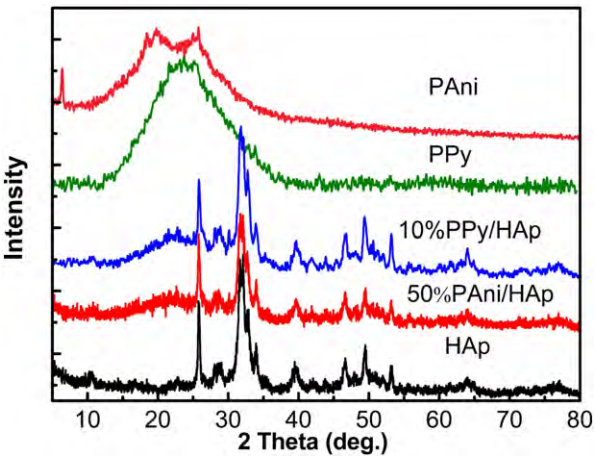

Fig. 2. XRD patterns of PAni, PPy, 10%PPy/HAp, 50%PAni/HAp and HAp.

of PPy is about 0.2 μm (Fig. 3(e)). The morphology of PPy is in accordance with other reports [20,23]. The PAni shows a tubular morphology, and the diameter is in the range of 70–100 nm (Fig. 3(c, e)). From the SEM images of PPy/HAp composite (g) and PAni/HAp composite (j), we can notice the existence of two parts of the composites, and it is not homogeneous enough at micro level. However, from the TEM images of the composites (h, i), it can be seen that the size of PPy and HAp is in accordance with that of pure HAp, PPy and PAni.

Fig. 4(a) shows the FT-IR spectra of pure PPy and PAni. For PPy, the specific adsorption bands are observed at 1473, 1187, and 1047 cm^{-1}, which correspond to the stretching vibration of C–N (1473 cm^{-1}, 1187 cm^{-1}) and in-plane deformation vibration of N–H (1047 cm^{-1}), respectively. For PAni, the characteristic bands at 1301 and 1147 cm^{-1} are observed, which correspond to the stretching mode of C–N in Ar–N (1301 cm^{-1}) and the vibration of the doped anion (1147 cm^{-1}), respectively. Fig. 4(b) exhibits the FT-IR spectra of pure HAp and the composites. For HAp, the specific peaks correspond to ν_4 PO_4^{3-} bending vibration mode (567, 603 cm^{-1}), ν_1 PO_4^{3-} stretching vibration mode (963 cm^{-1}), ν_3 PO_4^{3-} stretching vibration mode (1035, 1101 cm^{-1}), ν_2 bending mode of adsorbed water (1638 cm^{-1}, 3159, 3431 cm^{-1}) and ν_3 CO_3^{2-} asymmetric stretch vibration mode (1384 cm^{-1}) due to the reaction between HAp and CO_2, respectively [35] are observed. The composites show the specific bands of HAp, PPy and PAni, but some peaks slightly shift due to the interaction within the composite, and the intensity of the bands of PPy and PAni are relatively weaker due to the low mass content.

Fig. 5(a) presents the response–recovery curves of pure PPy to different concentrations of NH_3 from 50 ppm to 2000 ppm at room temperature. It can be seen obviously that the electric resistance of the sensor is at a relatively low level, indicating a high conductivity. When the sensor is exposed to ammonia, the electric resistance has a distinct increase. With the increase of the concentration, the electric resistance increases in a large magnitude, indicating an increased sensitivity. The PAni has a similar changing trend to the PPy, as shown in Fig. 5(b). PPy and PAni are p-type semiconductors whose carriers are the vacancies. NH_3, as a reducing gas, will donate electrons to PPy and PAni, resulting in a decrease of the density of the vacancy, so the electric resistance of PPy and PAni sensors will increase. With the increment of the NH_3 concentration, the volume of the absorbed NH_3 increases, so the sensitivity increases. But there is a slight shift of the initial resistance, that is to say, the resistance cannot recover to the original level, indicating some irreversible interactions between PPy (PAni) and NH_3. Furthermore, for PPy, the response time lasts several minutes, and the recovery time is as long as 20–30 min. The response/recovery time of PAni is relatively short, but still lasts several minutes. The highly

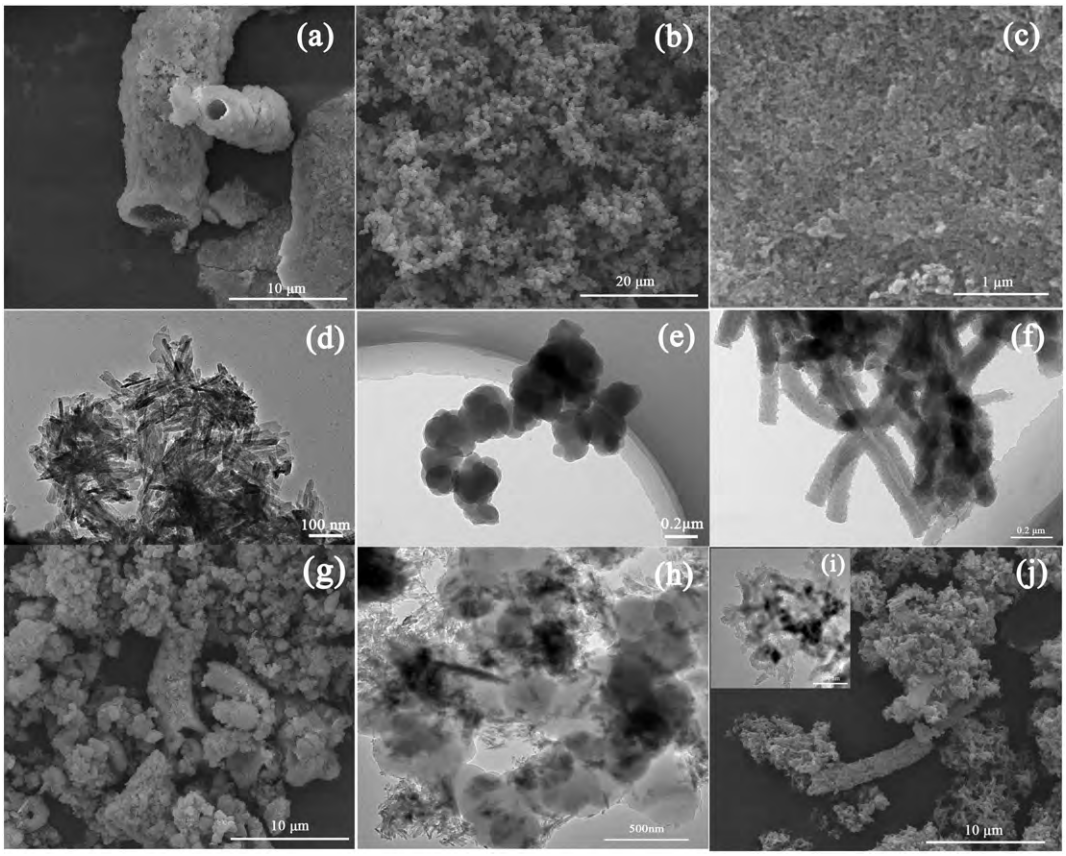

Fig. 3. SEM and TEM images of HAp (a, d), PPy (b, e), PAni (c, f), PPy/HAp composite (g, h), PAni/HAp composite (j, i).

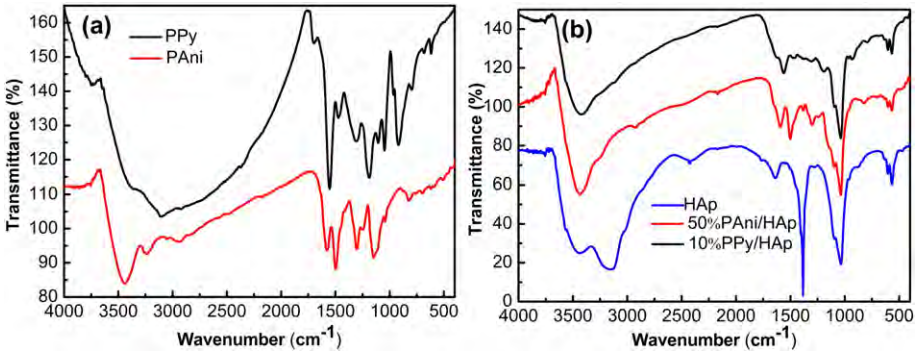

Fig. 4. FT-IR spectra of pure PPy and PAni (a) HAp, 10%PPy/HAp and 50%PAni/HAp (b).

ordered structures of PPy and PAni may cause the strong bonding and irreversible chemical adsorption between PPy (PAni) and NH_3 molecules.

The response sensitivity vs the concentration of NH_3 of pure HAp, PPy/HAp composites are presented in Fig. 6(a). It is obvious that 5%PPy/HAp shows the highest sensitivity to ammonia among all the samples. Compared to pure HAp, the sensitivity of 2.5%PPy/HAp is improved slightly. However, the sensitivity of 10%PPy/HAp composite is lower than those of 2.5%PPy/HAp and 5%PPy/HAp at any concentration, but still higher than that of pure HAp. It seems that only an appropriate content of PPy can improve the sensing properties to ammonia significantly. At the low concentrations from 10 ppm to 50 ppm, the increase of the sensitivity almost depends linearly on the concentration of ammonia. However, with the increase of the concentration from 50 ppm to 200 ppm, the increasing magnitude of the sensitivity becomes slow. At concentrations above 500 ppm, the sensitivity increases little, and tends to be saturated. It can be concluded that 10–50 ppm and 50–200 ppm are the linear ranges of PPy/HAp composites, the slope of the curve from 50 to 200 ppm is smaller than that from 10 to 50 ppm. It is favorable for the analysis of the gas species and gas concentrations since linear equations, which exhibits the correlations between sensitivities and gas concentrations, can be built up in the distinct linear ranges of the composites. Solving the equation groups is beneficial for analyzing the multicomponent gases. Although the detection limit need to be reduced in further study, PPy/HAp and PAni/HAp composites are promising sensing materials with high usability. Fig. 6(b) exhibits the response–recovery curves of 5%PPy/HAp composite from 5 ppm to 1000 ppm. The resistance of the composite decreases when it is exposed to ammonia, which is the same to HAp. Compared to pure PPy, the response time and the recovery time become shorter. The curves are not very stable. The reason may be that the sensors based on PPy/HAp composites are easy to be affected by slight environmental changes at low operation temperatures. Additionally, even at a low concentration of 5 ppm, the response value is still as high as 24.9%. Furthermore, the sensitivity increases with the increase of the concentration. When the concentration reaches 1000 ppm, the sensitivity almost gets saturated, near 90.7%.

Fig. 6(c) and (d) shows the sensing properties of PAni/HAp composites to ammonia. The sensitivity of the composites to ammonia is rather higher than that of the pure HAp, and the sensitivity of the composites increases with the increase of the mass percent of PAni from 1% to 20%. 20%PAni/HAp composite shows the best sensitivity to ammonia. Besides, the sensitivities of 30%PAni/HAp and 50%PAni/HAp are lower than that of 20%PAni/HAp, but higher than that of 1%PAni/HAp. The data of 30%PAni/HAp as well as 50%PAni/HAp are not shown here. With the increase of the concentration of ammonia, the sensitivity increases quickly in the beginning indicating that 50–100 ppm is the linear range of PAni/HAp composites, then tends to increase slowly and to saturate. The sensitivity of 20%PAni/HAp at 50 ppm is about 70%, and at 500 ppm, the sensitivity is about 85%. From Fig. 6(d), it can be seen clearly that the curves are smooth, indicating PAni/HAp composites are more stable than PPy/HAp. It is possible that the potential barrier existing between HAp and PPy is higher than that between HAp and PAni, which makes the signal not stable enough. Compared to PPy/HAp composites, the response/recovery time are shorter. The sensitivities of 5%PPy/HAp are higher than that of 20%PAni/HAp at every concentration.

Another four kinds of gases (n-heptane, ethanol, acetone and methanol) were chosen to study the selectivity of 20%PAni/HAp and 5%PPy/HAp composites. The data of 20%PAni/HAp at 100 ppm and the data of 5%PPy/HAp at 200 ppm are presented in Fig. 7. It is found that 20%PAni/HAp and 5%PPy/HAp composites exhibit the highest sensitivity to NH_3. The selectivity of a target gas to another gas can be characterized by the selectivity coefficient [23], which is defined as $K_{A/B} = S_A/S_B$. S_A and S_B are the sensitivities of a sensor to a target gas "A" and a interference gas "B", respectively. The higher the $K_{A/B}$ value, the better the selectivity. So the selectivity coefficients of ammonia to other gases for 20%PAni/HAp are in the range of 1.30–1.42, while the selectivity coefficients of ammonia

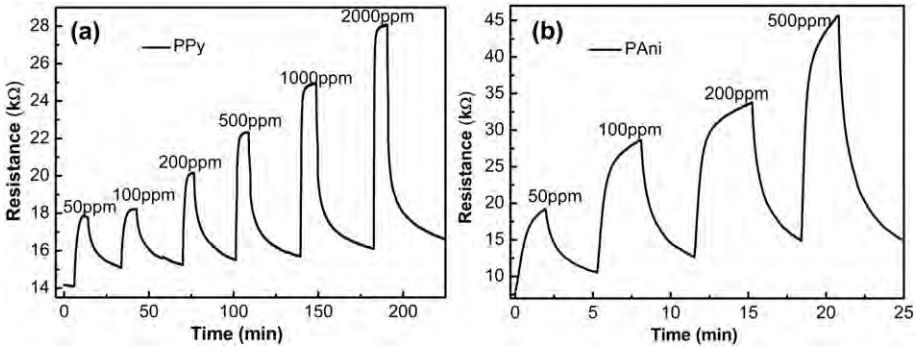

Fig. 5. Response–recovery curves of pure PPy (a) and PAni (b) to different concentrations of NH_3.

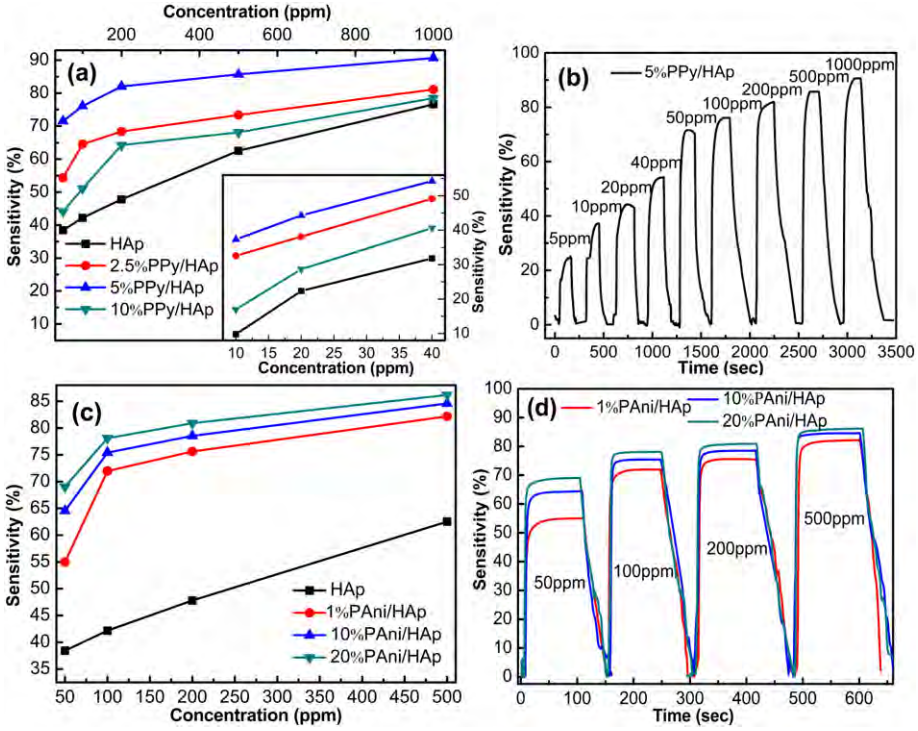

Fig. 6. Sensitivity vs ammonia concentration curves of PPy/HAp composites (a) and PAni/HAp composites (c) and response–recovery curves of PPy/HAp composites (b) and PAni/HAp composites (d).

to other gases for 5%PPy/HAp are in the range of 1.41–2.65. Therefore, 20%PAni/HAp and 5%PPy/HAp composites show higher selectivity to ammonia, and the selectivity of PPy/HAp is better than PAni/HAp.

Finally, the response time and the recovery time of pure PAni, HAp, PPy and PAni/HAp, PPy/HAp composites to ammonia at 200 ppm were calculated and shown in Fig. 8. It indicates that the response time of pure PPy and PAni to ammonia at 200 ppm are above 120 s, and the recovery time of PPy is above 900 s. The response time and the recovery time of pure HAp are about 20 s. After mixing with different mass percent of PAni, the response time does not change much, however, with the increasing of the mass percent of PAni, the recovery time of the composites increases. PPy/HAp composites with different mass percent of PPy have the similar response time of about 50 s. The recovery time of PPy/HAp increases with the increase of the mass percent of PPy. In general, the recovery time of the composites is several times of the response time, because the gas molecules need more time to diffuse out from the surface and pores of the composites. The response/recovery time of PPy/HAp is longer than those of PAni/HAp, since the response/recovery time of pure PPy is quite longer than pure PAni due to the strong interaction between gas molecules and PPy, as well as the highly ordered structure of PPy. But the response/recovery time of the composites is shorter than those of the pure polymers.

For understanding the enhanced sensing mechanism to ammonia, the conductive mechanisms of HAp, PPy and PAni should be mentioned firstly. HAp is considered to be a one-dimensional conductor whose charge carriers (protons) migrate along the c-axis from OH^- to the adjacent OH^- (Fig. 9(c)). The distance between the two adjacent OH^- is 0.344 nm, and is beyond the distance which the protons can hop. The distance between OH^- and its adjacent PO_4^{3-} (0.307 nm) is short enough to form a hydrogen bond [36], so the protons can penetrate along the path of $OH^- \rightarrow PO_4^{3-} \rightarrow OH^-$. Intrinsic PPy and PAni show very low conductivity. For protonic acid doped PPy and PAni, protons

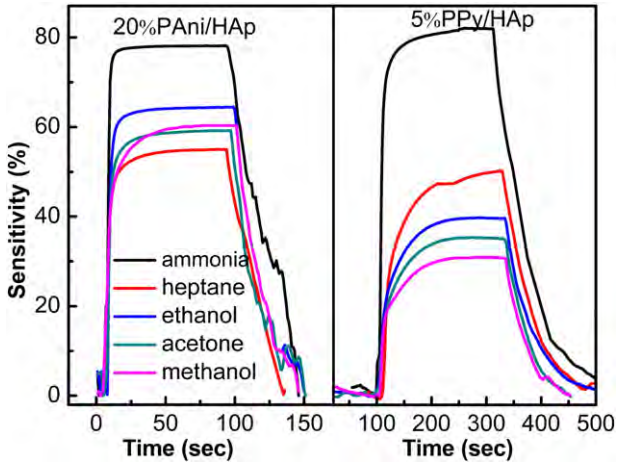

Fig. 7. Response–recovery curves of 20%PAni/HAp (100 ppm) and 5%PPy/HAp (200 ppm) composites to different kinds of gases.

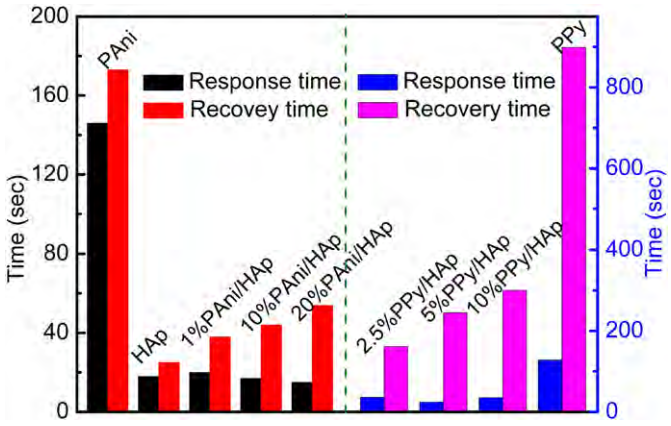

Fig. 8. Response time and recovery time comparison of pure PAni, HAp, PPy and PAni/HAp, PPy/HAp composites to ammonia at 200 ppm.

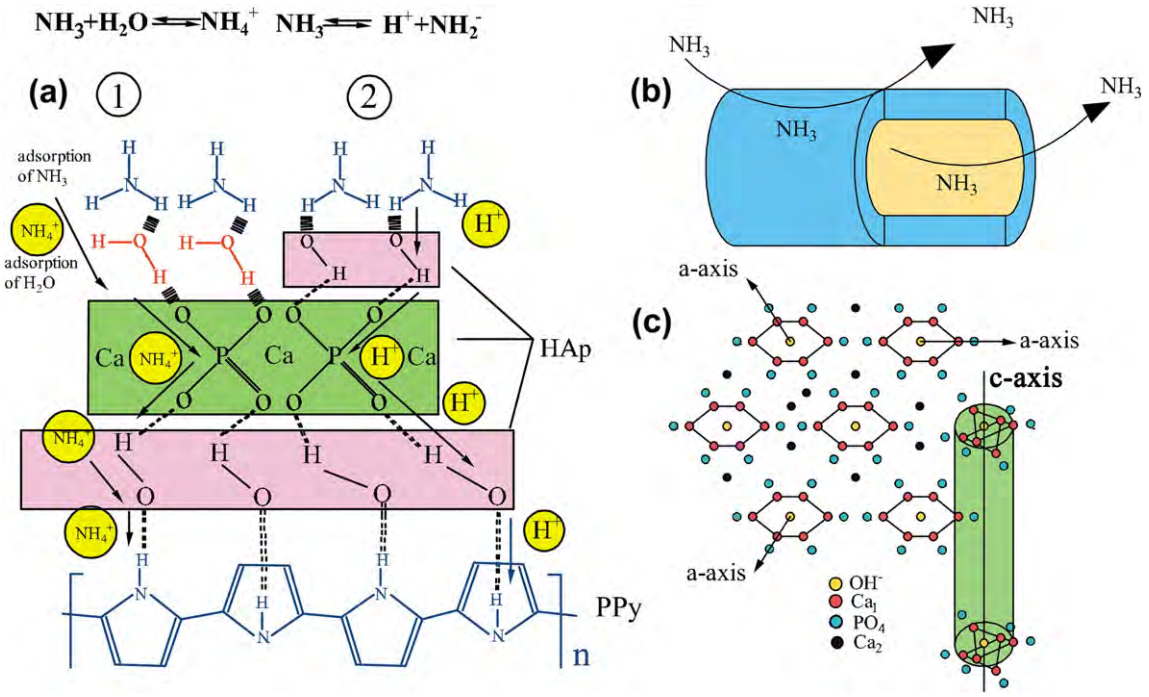

Fig. 9. Schematic diagram of sensing mechanism of PPy/HAp composites.

carrying positive charge transfer to the polymer molecule chains, resulting in the change of charge distribution state, so the conductivity of doped PPy and PAni increases significantly.

HAp behaves as an n-type semiconductor whose electric resistance decreases when exposing to reducing gases like NH_3. The sensing mechanisms of tubular HAp to ammonia has been proposed in Ref. [32]. PPy and PAni are p-type semiconductors, and their electric resistance increase in NH_3. The possible sensing mechanism of PPy/HAp composites to ammonia is illustrated as follows (the mechanism of PAni/HAp composites is almost the same):

Firstly, the electric conductivity of PPy is much higher than that of HAp. The electric current transfers preferably through the conductive PPy particles than HAp. So the electric resistance of the composite is lower than that of pure HAp [31].

Secondly, the doping content of protons in PPy is increased, so the electric resistance of the composite decreases. There are many functional groups, like –OH, acting as adsorption and reaction sites on the surface of tubular HAp. HAp serves as an anchor to capture NH_3 molecules (Fig. 9(b)). NH_3 molecules can dissociate to H^+ and NH_2^-. H^+ transfers along the path of $OH^- \rightarrow PO_4^{3-} \rightarrow OH^-$, and passes the hydrogen bond between OH^- of HAp and N–H of PPy. The doping level of H^+ in PPy increases due to the migration of protons from HAp to PPy, so the electric resistance of PPy decreases. Since the mass percent of PPy in the composite is small, it can be considered that PPy is wrapped up by HAp, and cannot contact with NH_3. The electric resistance of both parts of the composite decreases when the composite is exposed to NH_3 atmosphere. So the synergistic effects make the sensing properties of the composite to ammonia enhanced compared to pure HAp (② in Fig. 9(a)). Besides, HAp exhibits good hydrophilic behavior. PO_4^{3-} groups on the surface of HAp can form hydrogen bonds with H_2O molecules. The migration of H^+ in absorbed H_2O can improve the electric conductivity [37] of HAp at room temperature. NH_3 can also interact with H_2O and form hydrogen bonds. NH_4^+ can be formed as: $NH_3 + H_2O \rightarrow NH_3 \cdot H_2O \rightarrow NH_4^+ + OH^-$, and NH_4^+ transfers along the path of $PO_4^{3-} \rightarrow OH^-$ to the N–H position of PPy. So the doping level of protons in PPy can also be improved, and the electric resistance of PPy decreases. As a result, the sensing properties of the composites to ammonia are improved (① in Fig. 9(a)).

4. Conclusions

In summary, NH_3 sensors based on polymer (PPy, PAni)/hydroxyapatite composites were fabricated. The composites containing 5% PPy and 20% PAni exhibited the highest sensitivity to NH_3. The sensitivity of 5%PPy/HAp showed higher sensitivity and better selectivity than 20%PAni/HAp, but 20%PAni/HAp exhibited shorter response/recovery time and better stability. Besides, all composites possessed better reversibility and shorter response/recovery time than pure PPy and PAni. The enhanced sensing mechanisms to ammonia were proposed based on the conductivity of proton along the c-axis of HAp and the doping of H^+ in PPy and PAni. The synergistic effects between HAp and polymers make the polymer/hydroxyapatite composites very sensitive to ammonia at room temperature.

Acknowledgment

This research was financially supported by the National Natural Science Foundation of China (No. 51272289) and the Fundamental Research Funds for the Central Universities of Central South University (2015zzts180).

References

[1] B. Timmer, W. Olthuis, A. v. d. Berg, Ammonia sensors and their applications—a review, Sensors Actuators B Chem. 107 (2005) 666–677.
[2] G.K. Mani, J.B.B. Rayappan, A highly selective and wide range ammonia sensor—nanostructured ZnO: Co thin film, Mater. Sci. Eng. B 191 (2014) 41–50.
[3] M. Aslam, V. Chaudhary, I. Mulla, S. Sainkar, A. Mandale, A. Belhekar, K. Vijayamohanan, A highly selective ammonia gas sensor using surface-ruthenated zinc oxide, Sensors Actuators A Phys. 75 (1999) 162–167.
[4] B. Karunagaran, P. Uthirakumar, S. Chung, S. Velumani, E.K. Suh, TiO_2 thin film gas sensor for monitoring ammonia, Mater. Charact. 58 (2007) 680–684.
[5] K. Makhija, A. Ray, R. Patel, U. Trivedi, H. Kapse, Indium oxide thin film based ammonia gas and ethanol vapour sensor, Bull. Mater. Sci. 28 (2005) 9–17.
[6] D. Patil, L. Patil, P. Patil, Cr_2O_3-activated ZnO thick film resistors for ammonia gas sensing operable at room temperature, Sensors Actuators B Chem. 126 (2007) 368–374.
[7] M. Baghayeri, E.N. Zare, R. Hasanzadeh, Facile synthesis of PSMA-g-3ABA/MWCNTs nanocomposite as a substrate for hemoglobin immobilization: application to catalysis of H_2O_2, Mater. Sci. Eng. C 39 (2014) 213–220.

[8] M. Baghayeri, E.N. Zare, M. Namadchian, Direct electrochemistry and electrocatalysis of hemoglobin immobilized on biocompatible poly (styrene-alternative-maleic acid)/functionalized multi-wall carbon nanotubes blends, Sensors Actuators B Chem. 188 (2013) 227–234.
[9] M. Baghayeri, E.N. Zare, M.M. Lakouraj, Novel superparamagnetic PFu@ Fe_3O_4 conductive nanocomposite as a suitable host for hemoglobin immobilization, Sensors Actuators B Chem. 202 (2014) 1200–1208.
[10] M. Baghayeri, E.N. Zare, M.M. Lakouraj, A simple hydrogen peroxide biosensor based on a novel electro-magnetic poly (p-phenylenediamine)@Fe_3O_4 nanocomposite, Biosens. Bioelectron. 55 (2014) 259–265.
[11] M. Baghayeri, E.N. Zare, M.M. Lakouraj, Monitoring of hydrogen peroxide using a glassy carbon electrode modified with hemoglobin and a polypyrrole-based nanocomposite, Microchim. Acta 182 (2015) 771–779.
[12] M. Baghayeri, Glucose sensing by a glassy carbon electrode modified with glucose oxidase and a magnetic polymeric nanocomposite, RSC Adv. 5 (2015) 18267–18274.
[13] S.C. Hernandez, D. Chaudhuri, W. Chen, N.V. Myung, A. Mulchandani, Single polypyrrole nanowire ammonia gas sensor, Electroanalysis 19 (2007) 2125–2130.
[14] A. Kukla, Y.M. Shirshov, S. Piletsky, Ammonia sensors based on sensitive polyaniline films, Sensors Actuators B Chem. 37 (1996) 135–140.
[15] H. Kharat, K. Kakde, P. Savale, K. Datta, P. Ghosh, M. Shirsat, Synthesis of polypyrrole films for the development of ammonia sensor, Polym. Adv. Technol. 18 (2007) 397–402.
[16] M. Chougule, S. Pawar, S. Patil, B. Raut, P. Godse, S. Sen, V.B. Patil, Polypyrrole thin film: room temperature ammonia gas sensor, IEEE Sensors J. 11 (2011) 2137–2141.
[17] L. Geng, Gas sensitivity study of polypyrrole/WO_3 hybrid materials to H_2S, Synth. Met. 160 (2010) 1708–1711.
[18] L.N. G, S.R. W, P. Le, Y.Q. Z, S.M. Z, S.H. W, Preparation and gas sensitivity study of polypyrrole/tin oxide hybrid material, Chin. J. Inorg. Chem. 7 (2005) 977–981.
[19] J. Zhang, S. Wang, M. Xu, Y. Wang, H. Xia, S. Zhang, X. Guo, S. Wu, Polypyrrole-coated SnO_2 hollow spheres and their application for ammonia sensor, J. Phys. Chem. C 113 (2009) 1662–1665.
[20] L. Geng, Y. Zhao, X. Huang, S. Wang, S. Zhang, W. Huang, S. Wu, The preparation and gas sensitivity study of polypyrrole/zinc oxide, Synth. Met. 156 (2006) 1078–1082.
[21] K. Suri, S. Annapoorni, A. Sarkar, R. Tandon, Gas and humidity sensors based on iron oxide–polypyrrole nanocomposites, Sensors Actuators B Chem. 81 (2002) 277–282.
[22] K. Hosono, I. Matsubara, N. Murayama, S. Woosuck, N. Izu, Synthesis of polypyrrole/MoO_3 hybrid thin films and their volatile organic compound gas-sensing properties, Chem. Mater. 17 (2005) 349–354.
[23] S.R. Nalage, A.T. Mane, R.C. Pawar, C.S. Lee, V.B. Patil, Polypyrrole–NiO hybrid nanocomposite films: highly selective, sensitive, and reproducible NO_2 sensors, Ionics 20 (2014) 1607–1616.
[24] L.N. Geng, Gas sensitivity of polyaniline/SnO_2 hybrids to volatile organic compounds, Trans. Nonferrous Metals Soc. China 19 (2009) 678–683.
[25] L. Geng, Y. Zhao, X. Huang, S. Wang, S. Zhang, S. Wu, Characterization and gas sensitivity study of polyaniline/SnO_2 hybrid material prepared by hydrothermal route, Sensors Actuators B Chem. 120 (2007) 568–572.
[26] H. Tai, Y. Jiang, G. Xie, J. Yu, X. Chen, Fabrication and gas sensitivity of polyaniline–titanium dioxide nanocomposite thin film, Sensors Actuators B Chem. 125 (2007) 644–650.
[27] Y. Li, J. Gong, G. He, Y. Deng, Fabrication of polyaniline/titanium dioxide composite nanofibers for gas sensing application, Mater. Chem. Phys. 129 (2011) 477–482.
[28] H. Tai, Y. Jiang, G. Xie, J. Yu, X. Chen, Z. Ying, Influence of polymerization temperature on NH_3 response of PANI/TiO_2 thin film gas sensor, Sensors Actuators B Chem. 129 (2008) 319–326.
[29] S. Pawar, M. Chougule, S. Patil, B. Raut, P. Godse, S. Sen, V. Patil, Room temperature ammonia gas sensor based on polyaniline–TiO_2 nanocomposite, IEEE Sensors J. 11 (2011) 3417–3423.
[30] D. Dhawale, R. Salunkhe, U. Patil, K. Gurav, A. More, C. Lokhande, Room temperature liquefied petroleum gas (LPG) sensor based on p-polyaniline/n-TiO_2 heterojunction, Sensors Actuators B Chem. 134 (2008) 988–992.
[31] J. Gong, Y. Li, Z. Hu, Z. Zhou, Y. Deng, Ultrasensitive NH_3 gas sensor from polyaniline nanograin enchased TiO_2 fibers, J. Phys. Chem. C 114 (2010) 9970–9974.
[32] L. Huixia, L. Yong, T. Yanni, L. Lanlan, Z. Qing, L. Kun, T. Hanchun, Room temperature gas sensing properties of tubular hydroxyapatite, New J. Chem. 39 (2015) 3865–3874.
[33] Y. Zhang, K. Li, Q. Zhang, W. Liu, Y. Liu, C.E. Banks, Multi-dimensional hydroxyapatite (HAp) nanocluster architectures fabricated via nafion-assisted biomineralization, New J. Chem. 39 (2015) 750–754.
[34] Y. Zhang, Y. Liu, X. Ji, C.E. Banks, W. Zhang, Sea cucumber-like hydroxyapatite: cation exchange membrane-assisted synthesis and its application in ultra-sensitive heavy metal detection, Chem. Commun. 47 (2011) 4126–4128.
[35] P. Kanchana, C. Sekar, EDTA assisted synthesis of hydroxyapatite nanoparticles for electrochemical sensing of uric acid, Mater. Sci. Eng. C 42 (2014) 601–607.
[36] K. Yamashita, K. Kitagaki, T. Umegaki, Thermal instability and proton conductivity of ceramic hydroxyapatite at high temperatures, J. Am. Ceram. Soc. 78 (1995) 1191–1197.
[37] M. Nagai, T. Nishino, Surface conduction of porous hydroxyapatite ceramics at elevated temperatures, Solid State Ionics 28 (1988) 1456–1461.